

Geochemistry, Geophysics, Geosystems®



RESEARCH ARTICLE

10.1029/2023GC011137

Key Points:

- New Ar-Ar plagioclase dates and chemical data from the Malwa Plateau on the northern margin of the Deccan LIP
- Data invalidate correlation to stratigraphy in the Western Ghats
- Data support the presence of multiple eruptive centers for the Deccan LIP

Supporting Information:

Supporting Information may be found in the online version of this article.

Correspondence to:

A. J. Tholt,
andrewtholt@berkeley.edu

Citation:

Tholt, A. J., Renne, P. R., Marzoli, A., Vanderkluyzen, L., Mohabey, D., Samant, B., et al. (2023). Geochronological constraints on the evolution and petrogenesis of the Malwa Plateau subprovince of the Deccan Traps. *Geochemistry, Geophysics, Geosystems*, 24, e2023GC011137. <https://doi.org/10.1029/2023GC011137>

Received 24 JUL 2023

Accepted 1 NOV 2023

Geochronological Constraints on the Evolution and Petrogenesis of the Malwa Plateau Subprovince of the Deccan Traps

A. J. Tholt¹ , P. R. Renne^{1,2}, A. Marzoli³ , L. Vanderkluyzen⁴ , D. Mohabey⁵, B. Samant⁵, A. Dhobale⁶, K. Pande⁷, and S. Self¹

¹Department of Earth and Planetary Science, University of California, Berkeley, Berkeley, CA, USA, ²Berkeley Geochronology Center, Berkeley, CA, USA, ³Dipartimento Territorio e Sistemi Agro-Forestali, Università di Padova, Legnaro, Italy, ⁴Department of Biodiversity, Earth & Environmental Science, Drexel University, Philadelphia, PA, USA, ⁵Department of Geology, RTM Nagpur University, Nagpur, India, ⁶Department of Geology, Savitribai Phule Pune University, Pune, India, ⁷Department of Earth Sciences, Indian Institute of Technology Bombay, Mumbai, India

Abstract The eruptive history of the Malwa Plateau Subprovince of the Deccan Traps is addressed by dating 21 lavas spanning the exposed stratigraphic extent, using the ⁴⁰Ar/³⁹Ar method applied to plagioclase separates. Major, minor, and trace element geochemistry was determined for each of the dated lavas and four additional ones. Dating results indicate that the eruptions began prior to 66.8 Ma, at least 400 ka before the oldest known lava in the more extensively studied Western Ghats, representative of the main Deccan province, to the south. Eruption rates peaked from 66.4 to 66.3 Ma and then diminished until 65.6 Ma. The peak in eruption rates coincides with the well-documented Late Maastrichtian Warming event. Malwa lavas show some major and trace element affinities with geochemically defined lava flow formations of the Western Ghats, but are generally out of the stratigraphic sequence manifest in the Western Ghats. The distinct geochemical evolution of Malwa Plateau lavas compared with those of the Western Ghats is at least in part a consequence of differences in crustal composition between the two subprovinces. Modeling of REE concentration patterns of Malwa lavas suggests that they were derived by slightly lower degrees of partial melting, at lower mantle temperatures and depths, than those in the Western Ghats. The Malwa Plateau thus appears to record an earlier, cooler stage of the Deccan plume's evolution and continued to erupt through a large part of the lifetime of the main Deccan province.

1. Introduction

The Deccan Traps volcanic province of India is an iconic Large Igneous Province (LIP) that covers more than 500,000 km² with an estimated present-day volume of about 600,000 km³ (Jay & Widdowson, 2008; Kale et al., 2020; Krishnamurthy, 2020; Richards et al., 2015; Verma & Khosla, 2019). Composed predominantly of tholeiitic basalt, the stratigraphic sequence of lavas exceeds 1 km in some locations, with an inferred aggregate thickness of ~3 km (Ray et al., 2007). The LIP is divided into subprovinces (Figure 1), with a majority of studies centered around the extensive exposures of the N-S trending Western Ghats escarpment, representative of the main Deccan province. A systematic geochemical stratigraphy recorded in the Western Ghats (WG) (e.g., Beane et al., 1986) is often used as a reference to correlate distal outcrops as well as outlying subprovinces to the main exposures.

Despite the wealth of knowledge that has come from studies based in the WG, there remains a need for fundamental data from outlying subprovinces to understand the spatial-temporal and petrological evolution of the Deccan Traps magmatic system as a whole. The assumption that the chemical stratigraphy adopted by many for the Western Ghats (e.g., Beane et al., 1986) is applicable to various other subprovinces remains testable and unresolved. Several studies have questioned this notion (e.g., Kale et al., 2020; Mittal & Richards, 2021; Peng et al., 1998; Self et al., 2022; Sheth et al., 2013) arguing that regional variations in chemical stratigraphy indicate multiple eruptive centers with independent magmatic evolution trends. Another first-order question is whether Deccan magmatic activity proceeded from north to south, as suggested by studies of intrusive complexes in the northern extremes of the LIP (e.g., Basu et al., 1993), or not, as concluded by Parisio et al. (2016). The evidence of a spatial age progression would be consistent with northward motion of the Indian plate over a mantle plume, albeit subject to constraints of the plume head dimensions, the permeability of the lithosphere, Indian plate

© 2023 The Authors. Geochemistry, Geophysics, Geosystems published by Wiley Periodicals LLC on behalf of American Geophysical Union. This is an open access article under the terms of the Creative Commons Attribution-NonCommercial-NoDerivs License, which permits use and distribution in any medium, provided the original work is properly cited, the use is non-commercial and no modifications or adaptations are made.

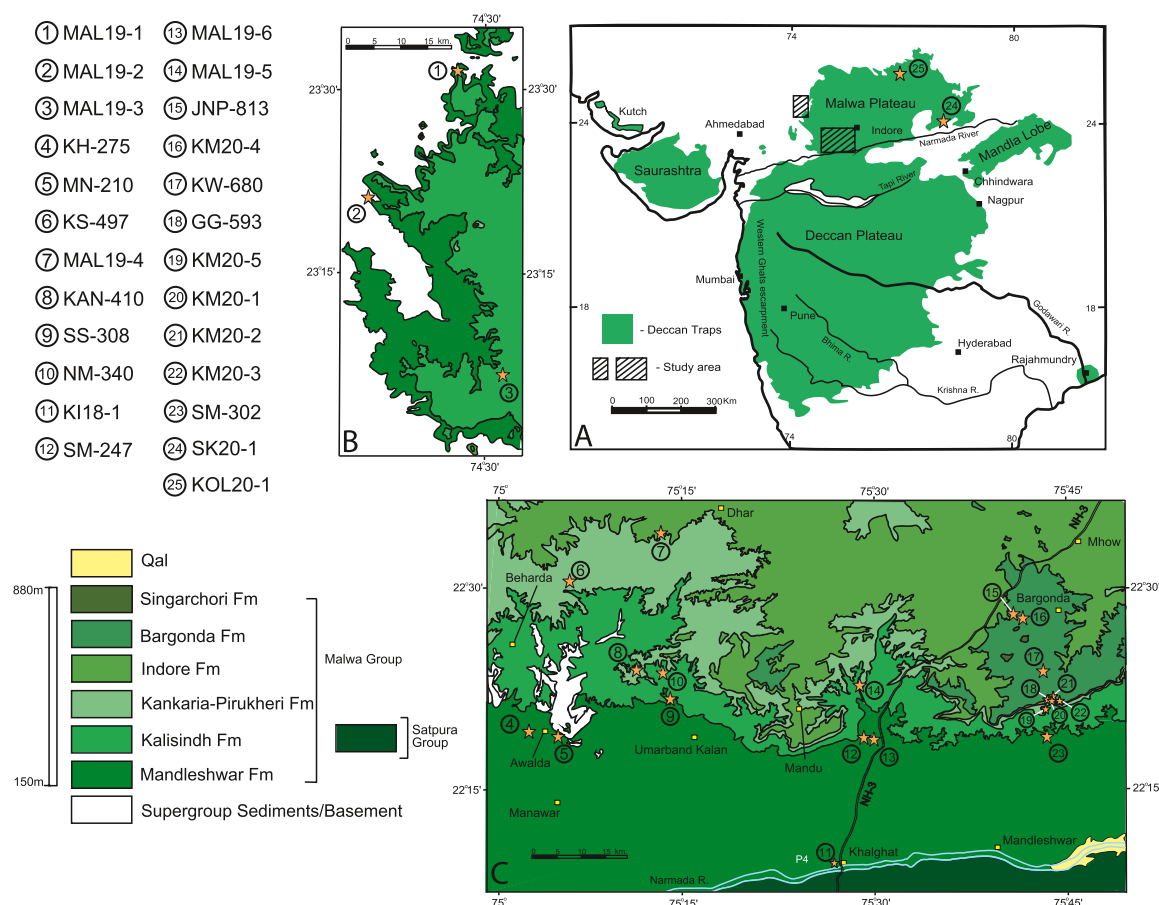


Figure 1. (a) Schematic map of the Deccan Traps Large Igneous Province, India. Numbered sample locations are marked with stars, and the coordinates for samples are listed in Table 1. Patterned rectangular insets mark the locations of geologic maps B and C. (b) 1:50,000 scale geologic map of a western portion of the Malwa Plateau modified from GSI mapping, 1993. (c) 1:50,000 scale geologic map of southern Malwa Plateau modified from GSI mapping, 1993.

velocity, and the rate and the extent of lateral plume head expansion over time. Here, we present new geochemical and $^{40}\text{Ar}/^{39}\text{Ar}$ geochronological data for lavas from the MP, at the northern edge of the province, toward a more comprehensive understanding of the petrologic evolution and tempo of Deccan eruptions overall.

The Deccan Traps were the first continental LIP to have been invoked as a driver of mass extinctions and/or periods of major ecological change (Callegaro et al., 2023; Courtillot et al., 1986; McLean, 1985). The relationship of Deccan magmatic activity with the Cretaceous–Paleogene boundary (KPB) extinctions remains ambiguous and warrants continued investigation. The Deccan Traps are one of the largest and youngest continental LIPs, and are thus comparatively well exposed and preserved, as is the stratigraphic record of contemporaneous geologic events (Sprain et al., 2015). An emerging body of evidence from diverse observations suggests that environmental changes perturbed the biosphere in the Late Maastrichtian, roughly coincident with the onset of volcanism in the Western Ghats. Dinosaur fossils from associated Deccan intertrappean sediments are absent for at least 350 ka leading up to the KPB (Mohabey & Samant, 2013). Oxygen isotope data from benthic foraminifera indicate warming by $\sim 4^\circ\text{C}$ beginning around 66.3–66.4 Ma and peaking at about 66.2 Ma (Barnet et al., 2018; Hull et al., 2020); this warming event is anomalously intense compared with expected orbitally modulated climate effects (Westerhold et al., 2020). Studies of North America's terrestrial sedimentary record suggest a temperature increase in the same magnitude, as well as increased pCO_2 and baseline mercury approximately coincident with the marine warming event (e.g., Fendley et al., 2019; Tobin et al., 2014; Wilf et al., 2003; Wilson, 2005). Voluminous ($>10^6 \text{ km}^3$) basaltic eruptions are a plausible explanation for globally recognized Late Maastrichtian changes through the injection of climate altering gases (Self et al., 2006), but require strong links between potential ecological forcing and the timing of volcanism if the gases are emitted by eruptions or passive degassing (Hernandez Nava et al., 2021; Mittal & Richards, 2021; Self et al., 2022; Sprain et al., 2019) of magma or volatile-rich country rocks.

Table 1
Coordinates, Elevations, and Ages for All Samples in This Study

	Lat. (°N)	Long. (°E)	Elev (m)	Age (Ma)	$\pm\sigma^1$	$\pm\sigma^2$
KI18-1	22.1505	75.4406	134	66.834	0.075	0.077
MN-210	22.3224	75.0896	210	Not dated		
MAL19-2	23.3533	74.3279	230	66.514	0.141	0.146
SM-247	22.3122	75.4941	247	Not dated		
MAL19-6	22.3116	75.4965	249	66.549	0.072	0.082
KH-275	22.3224	75.0527	275	66.427	0.097	0.106
SM-1-302	22.5686	75.7195	302	66.341	0.114	0.121
SS-308	22.3787	75.2306	308	66.393	0.108	0.118
NM-340	22.4021	75.2526	340	Not dated		
MAL19-1	23.5221	74.4605	370	66.350	0.058	0.072
MAL19-5	22.3786	75.4807	394	66.272	0.111	0.120
MAL19-3	23.1062	74.5269	410	66.348	0.123	0.132
KAN-410	22.4029	75.1932	410	66.352	0.108	0.115
KM20-1	22.3580	75.7245	490	66.351	0.094	0.103
KS-497	22.5091	75.1055	497	66.349	0.144	0.150
MAL19-4	22.5683	75.2257	551	66.236	0.078	0.089
KM20-2	22.3604	75.7242	575	66.387	0.078	0.089
GG-593	22.3620	75.7252	593	66.242	0.104	0.113
KM20-3	22.3585	75.7335	664	Not dated		
KM20-5	22.4650	75.6777	673	66.091	0.106	0.115
KW-680	22.4032	75.7145	680	66.164	0.081	0.090
JNP-813	22.4642	75.6859	813	65.868	0.134	0.140
KM20-4	22.4615	75.6881	835	65.796	0.117	0.123
SK20-1	23.4247	78.6226	558	65.733	0.055	0.069
KOL20-1	25.1864	77.4614	447	66.829	0.092	0.102

Note. Ages calculated with calibration of Renne et al. (2011). σ^1 age uncertainty include analytical sources only. σ^2 age uncertainty include systematic sources from decay constants and isotopic data for standard.

Resolution of the issues outlined here is dependent to a variable extent on precise and accurate geochronology. Attempts at dating the duration of Deccan volcanism have been presented over several decades utilizing $^{40}\text{K}/^{40}\text{Ar}$ (Alexander, 1981; Chenet et al., 2007; Kaneoka & Haramura, 1973; Wellman & McElhinny, 1970), $^{40}\text{Ar}/^{39}\text{Ar}$ (Chenet et al., 2007; Courtillot et al., 1988; Duncan & Pyle, 1988; Hofmann et al., 2000; Hooper et al., 2010; Pande et al., 2004; Renne et al., 2015; Schöbel et al., 2014), magnetostratigraphic (Schöbel et al., 2014; Vandamme et al., 1991), and U-Pb (Eddy et al., 2020; Schoene et al., 2019) data sets. More recent constraints on the timing of Deccan main phase volcanism as well as the likely location of the KPB within the stratigraphy (Schoene et al., 2019; Sprain et al., 2019) have vastly improved the time frame that is relevant to the relationship between the Deccan Traps and the KPB. Nonetheless, current age resolution permits only coarse climate modeling via geochemical box models (e.g., Zeebe, 2012), and there are differences in the tempo of eruptions inferred by Schoene et al. (2019) versus Sprain et al. (2019).

2. The Malwa Plateau

The Malwa Plateau is a physiographic region whose name has been widely used to denote a subprovince of the Deccan Traps. Within this subprovince, the basaltic lavas that are clearly part of the overall LIP are assigned to seven formations comprising the Malwa Group as lithostratigraphically defined by Geological Survey of India (1993). Occurrences of Malwa Group lava outcropping over the MP are bounded to the south by the Narmada River and are generally north of the ENE–WSW trending Son–Narmada–Tapti Lineament zone, referred to herein as the Narmada Rift (Figure 1). The Narmada Rift marks a recurrent and long-lived boundary which divides Peninsular India into geologically distinct crustal and lithospheric provinces (Shanker, 1991; Valdiya & Sanwal, 2017). Within the Malwa Plateau, Deccan lavas variably overlie the Proterozoic intracratonic terrigenous, shale, and carbonatic strata of the Bijawar Group and the Vindhyan Supergroup (Singh & Chakraborty, 2022), with the Archean Bundelkhand craton forming a local basement. By contrast, the crustal basement for Western Ghat lavas where exposed is predominantly plutonic or metamorphic crystalline rocks.

The current areal extent and volume of the Malwa Plateau magmatic rocks are estimated to be 80,000 km² and 21,000 km³, respectively (Schöbel et al., 2014). Exposed Malwa lava sections are thickest toward the southern

margin of the plateau with the highest present-day peaks roughly 850 m above sea level. At the southern margin, the basal contact of Deccan basalts is not exposed, but as much as ~800 m of lavas in the subsurface has been inferred from gravity and seismic studies (Verma & Banerjee, 1992). If the subsurface extent of lavas around the Narmada Rift is near the upper inferred limit, the total present volume of Malwa lavas probably exceeds the amount estimated by Schöbel et al. (2014), who assumed an average thickness of 300 m. In any case, we regard the 21,000 km³ volume estimate as a minimum value for the original (pre-erosional) volume of extruded lava.

Schöbel et al. (2014) used the anisotropy of magnetic susceptibility to infer that Malwa Group lavas flowed northward and concluded that the eruptive center(s) were within the Narmada Rift. This is supported by an abrupt thickening of the lava sequence as the Narmada Rift is approached from the north, although the original thickness of the lava sequence in the northern Malwa Plateau is unknown. However, the minimum ~200 m thickness of lavas assigned to magnetic polarity subchron C30N in a southern transect is approximately twice the maximum thickness of this subchron in two other transects to the northwest (Schöbel et al., 2014). In all these transects, lavas assigned to the Maastrichtian subchron C30N are overlain by reverse polarity lavas of C29R; hence, the implied southward thickening trend is immune to the vagaries of subsequent erosion. Schöbel et al. (2014) recognized normal faults within the most western and northwestern regions of the Malwa Plateau though they do not exhibit significant offset and do not appear to invalidate the general thickening trend to the south.

Some previous studies of Malwa basalts were focused on the paleomagnetic stratigraphy (e.g., Bhalla & Rao, 1974; Khadri, 2003; Khadri & Nagar, 1994; Schöbel et al., 2014) and revealed a normal-reverse-normal polarity sequence spanning Chrons 30N–29R–29N. These data along with a plagioclase $^{40}\text{Ar}/^{39}\text{Ar}$ age of 67.10 ± 0.22 Ma (Schöbel et al., 2014; recalculated to the Renne et al., 2011 calibration) suggested that the Malwa Plateau records an older history than that known in the Western Ghats where generally only Chrons 29R–29N are clearly represented. Eddy et al. (2020) dated zircons by U–Pb that were extracted from seven Malwa Plateau red bole horizons (saprolite layers between lava flows) based on the same approach and methodology as used in the Western Ghats by Schoene et al. (2019). The premise underlying this approach is that the zircons were deposited by ash fall from distal explosive eruptions during hiatuses between lava extrusions, and they thus date lava emplacement. Preferred model ages reported by Eddy et al. (2020) range from 66.375 to 66.137 Ma, largely overlapping the ages of the older (i.e., Kalsubai and Lonavala Subgroups) lavas of the Western Ghats.

3. Samples and Methods

In order to directly constrain the timing and chemistry of Malwa lavas, we collected 25 lava samples from outcrops predominately in the southern region where sections are not perceptibly faulted and expose the maximum range of elevations at which lava is exposed. All of the samples are plagioclase-phyric, with plagioclase phenocrysts ranging from ~0.5 to 10 mm in dimension, commonly occurring in glomerocrysts. Clinopyroxene is also present as a phenocryst phase, as is olivine, which is ubiquitously replaced by secondary alteration products. Four of these samples proved unsuitable for $^{40}\text{Ar}/^{39}\text{Ar}$ dating due to the abundance of inclusions within plagioclase or the extent of alteration of the plagioclase observed during mineral separation. Seven of the samples are plagioclase megacrystic basalts whose geochemistry has been presented previously (Marzoli et al., 2022). Coordinates for all samples are given in Table 1.

Plagioclase separates from the 21 samples selected for dating were handpicked to purity after being crushed in a disk mill, sieved, magnetically separated, and cleaned ultrasonically for less than 2 min in a 5% hydrofluoric acid solution. Samples were co-irradiated in Al disks along with Fish Canyon sanidine neutron fluence monitors in four separate 7 hr irradiations in the Cadmium-Lined In-Core Irradiation Tube (CLICIT) facility of the Oregon State University TRIGA reactor. Neutron fluence (i.e., J -value) for each sample was determined by a planar interpolation between three bracketing standard positions. Four to eight ca. 20–40 mg aliquots of plagioclase from each sample were analyzed at the Berkeley Geochronology Center in replicate 12–15 step incremental CO_2 laser heating experiments using a MAP 215C mass spectrometer. Weighted mean plateau ages are based on the calibration of Renne et al. (2011) and are summarized in Table 1. Full isotopic data and relevant meta-data are given in Tables S1 and S2. Age models for the Malwa Plateau were produced using sample elevations combined with 2σ weighted mean plateau ages, including systematic uncertainties, using the Chron.jl software package (Keller, 2018).

Whole rock major and trace element chemical data were obtained on all 25 samples through X-ray fluorescence spectrometry (XRF) and inductively coupled plasma mass spectrometry (ICP-MS) analyses at the GeoAnalytical Lab at Washington State University and are presented in Tables S3 and S4. Data from XRF and ICP-MS analyses were compared with Western Ghats chemotypes via discriminant-function analysis (DFA) using the SPSS v.27 software for Macintosh following Peng et al. (1998) and Vanderkluyzen et al. (2011). Sample formation designations used herein for the Malwa Group follow the nomenclature established by the Geological Survey of India (Figure 1) which are based on field criteria rather than geochemistry.

4. Results

4.1. Geochronology Results

All samples selected for $^{40}\text{Ar}/^{39}\text{Ar}$ dating yielded replicate age plateaus (Figure 2) defined by >65%, and mostly >90%, of the ^{39}Ar released. Plateaus are defined by contiguous steps that are mutually indistinguishable at 95% from their inverse variance-weighted mean considering only analytical uncertainties. Replicate incremental heating analyses yielded plateau ages that are mutually indistinguishable at 95% confidence. Ca/K ratios are relatively constant for each sample and range from ~20 to ~200, as is consistent with Ca/K obtained by electron microprobe on Malwa plagioclase megacrysts (Marzoli et al., 2022). As expected, samples with relatively low Ca/K, particularly the plagioclase megacryst bearing samples, yielded the most precise plateau ages.

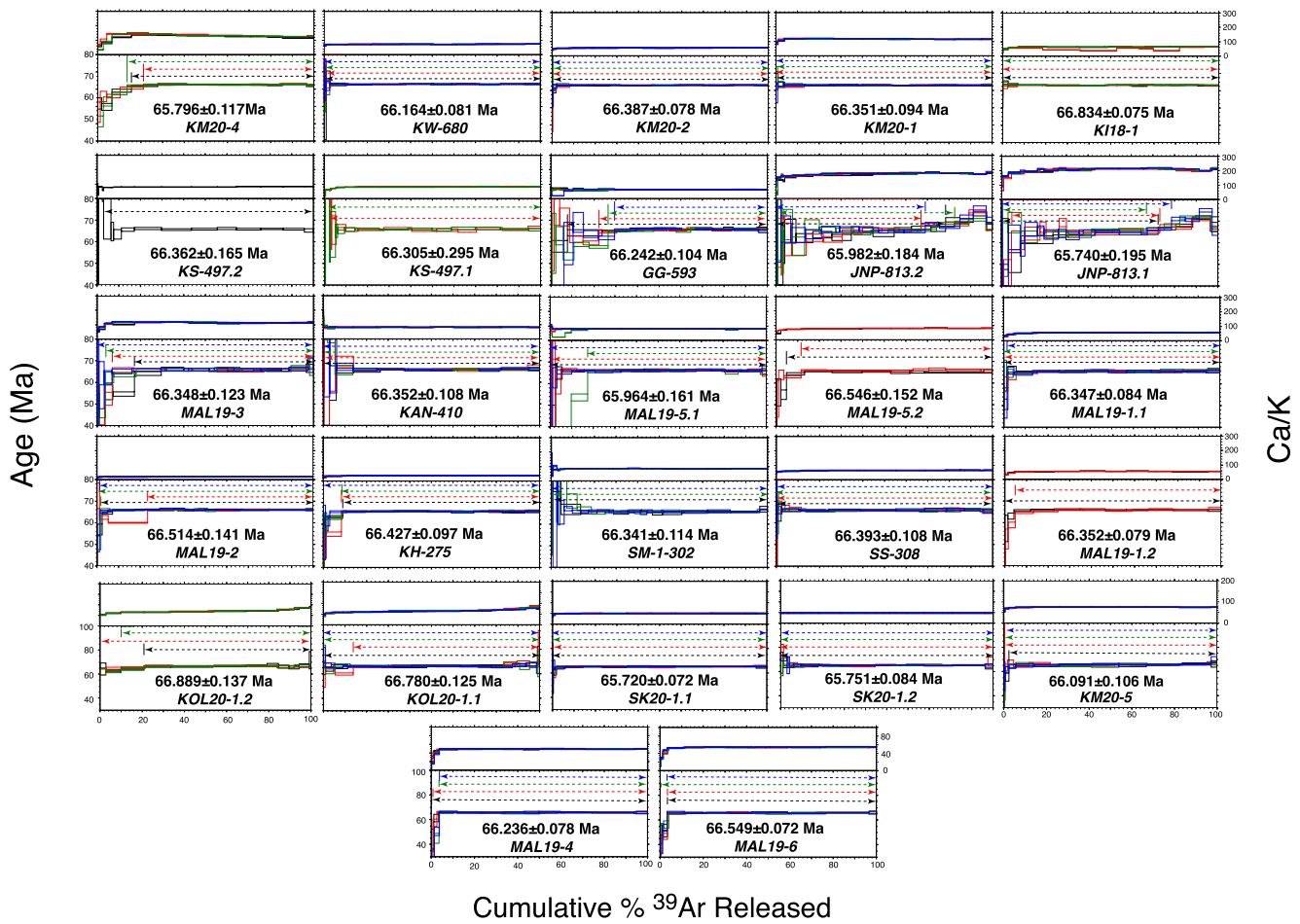


Figure 2. $^{40}\text{Ar}/^{39}\text{Ar}$ age spectra for Malwa Plateau basalt samples presented in this study. The lower panel of each plot shows 1–4 age spectra from step-heating analyses of multi-grain plagioclase aliquots from a given irradiation position shown by the laboratory identification number (LID#) at the bottom. The upper panel depicts the Ca/K spectrum matched by color to the corresponding age spectrum. Steps defining age plateaus are indicated by horizontal bars. Dashed lines with arrows indicate the extent of age plateaus for each step-heated aliquot. The weighted mean plateau age for each LID# is shown with 1σ analytical uncertainty limits.

Results show that lavas currently exposed in the southern MP spanning 700 m in elevation record roughly 1 million years of eruptive history. Eruptions began as early as 66.834 ± 0.075 Ma (1σ analytical uncertainty) as indicated by the weighted mean plateau age for sample KI18-1 of the Mandleshwar Formation, sampled a few meters above the Narmada River representing the lowest exposed lava in this vicinity. This age is significantly older than the oldest high-precision age of 66.413 ± 0.067 Ma (Sprain et al., 2019) in the Jawhar Formation of the Western Ghats lavas (Jawhar Formation) and extends the initiation of Deccan volcanism by ca. 400 ka. Ages for lavas of the upper Mandleshwar through the Bargonda Formations (~200–700 m elevation) indicate that Malwa volcanism entered a ~350,000 years-long interval of quasi-continuous eruptions leading up to the Cretaceous–Paleogene boundary. The eruption tempo likely declined from this frequency as implied by the two youngest and stratigraphically highest samples JNP-813 at 813 m above sea level (masl) and KM20-4 at 843 masl of the Singarchori formation. Our age model (Figure 3) clearly shows a lower lava accumulation rate at the base and top of the exposed section, which is consistent with a magma production rate that initially ramps up to maximum and then ramps down again. The duration of the waxing and waning phases of eruption rate are poorly constrained due to the unknown extent of erosion in this region and the undated section of lavas below the lowest dated flow at the Narmada River.

Two of the dated samples occur sufficiently far from the southern escarpment of the Malwa Plateau that they cannot be confidently placed in the age model. The first sample, KOL20-1 occurs at 447 masl in the northernmost extremity of the Malwa Plateau where several isolated erosional remnants of basalt unassigned to formations overlie the Proterozoic Vindhyan sedimentary strata. Its age (66.829 ± 0.092 Ma) is indistinguishable from that

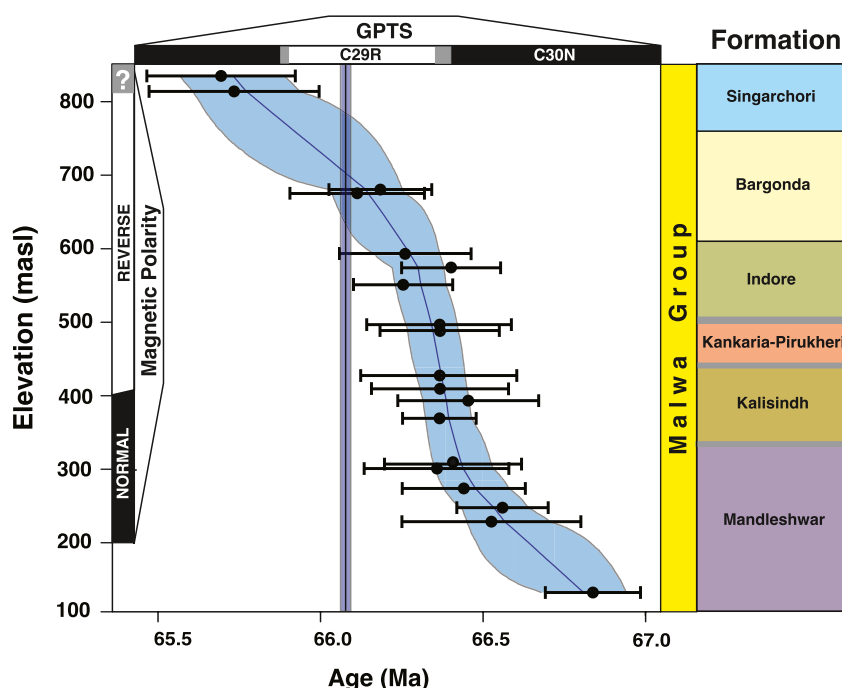


Figure 3. Age versus elevation for Malwa Plateau basalt samples. $^{40}\text{Ar}/^{39}\text{Ar}$ ages plotted as a function of elevation, showing age model with 95% confidence region. Uncertainties for data points are 2σ , excluding systematic sources. Ages and uncertainties (gray bars) for geomagnetic polarity time scale (GPTS) are from Sprain et al. (2018). Magnetic polarity zonation for the Malwa Plateau from Schöbel et al. (2014). Stratigraphy of the Malwa group follows usage by the Geological Survey of India. Vertical purple bar denotes the KP at 2σ uncertainty, data taken from Sprain et al., 2015.

of the lowermost exposed lava (KI18-1) to the south, though its composition is quite different (Table S2b). If this northern Malwa lava was erupted from the Narmada Rift zone, its elevation higher than sample KI18-1 implies a significant amount of post eruptive subsidence of the southern Malwa Plateau. It is unlikely, however, that these temporally correlative though geochemically distinct lavas erupted from the same vent or fissure.

The second sample, SK20-1, occurs near the easternmost extremity of the Malwa Plateau, where the unit outcrops in isolated occurrences lacking stratigraphic context. It has been previously assigned to the Kankaria-Pirukheri or Indore Formations (GSI, 1993), but its age (65.733 ± 0.055 Ma) is much younger than any of the lavas (i.e., samples KM20-1, KS-497, MAL19-4, KM20-2, and GG-593) between 450 and 620 m elevation assigned to these same formations in the southern Malwa Plateau (e.g., as shown in Figure 3) whose average age is 66.31 ± 0.07 Ma.

4.2. Geochemistry Results

All but one of the samples analyzed are tholeiitic basalts or basaltic andesites with SiO_2 ranging from 49.3 to 54.2 wt% on a volatile-free basis. Except for the topmost sample JNP-813 ($\text{TiO}_2 = 0.99$ wt%; $\text{FeO} = 10.8$ wt%; $\text{MgO} = 6.8$ wt%), all samples are high in TiO_2 (2.3–3.3 wt%) and FeO (10.7–15.7 wt%) and low in MgO (3.8–6.9 wt%). The generally low MgO contents suggest that none of the analyzed basalts have a composition consistent with a primary mantle melt. Trace element contents and ratios show significant differences among the studied rocks. For example, the topmost sample JNP-813 stands out because of its generally low trace element contents (e.g., La 11.4, Nb 5.1 ppm) and low LREE/HREE (e.g., La/Lu = 24.7) and Ba/Nb (22.6). The one alkaline basalt analyzed and dated in this study (MAL19-2; 66.51 ± 0.28 Ma) is classified as trachybasalt and was sampled from 230 m elevation at the western extremity of the Malwa Plateau. This sample is distinctive in trace element chemistry, including strong LREE/HREE enrichment (La/Lu = 109.6), significantly higher than those of the sub-alkaline tholeiitic basalts of the Malwa Plateau. This sample also contains high K_2O and K/Na (it is potassic as $\text{Na}_2\text{O}-\text{K}_2\text{O} < 2.0$ wt%), a significant enrichment of all incompatible trace elements, and a positive Nb-Ta anomaly on a mantle-normalized multi-element diagram (normalized after Sun and McDonough (1989)) while the tholeiitic

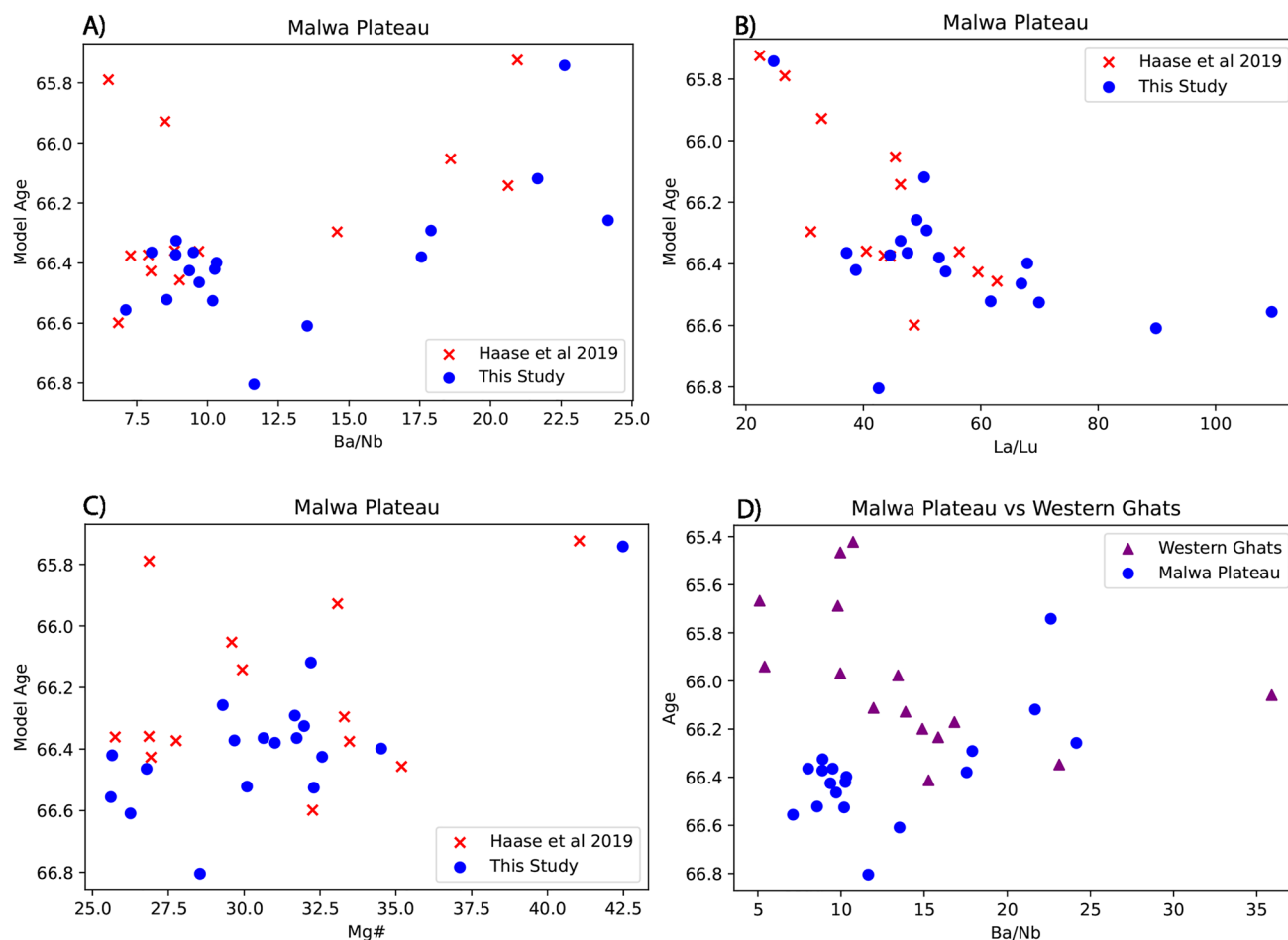


Figure 4. (a) Ba/Nb versus model ages from this study and data from Haase et al. (2019). (b) La/Lu versus model ages from this study and data from Haase et al. (2019). (c) Mg# versus model ages from this study and Haase et al. (2019) (d) Ba/Nb versus ages of Western Ghats samples from Sprain et al. (2019) and model ages from this study.

basalts always show a negative Nb anomaly (Sun et al., 1979). Overall, our major, minor, and trace element data overlap substantially with those of Haase et al. (2019) for the Malwa Plateau (Figure 4). Haase et al. (2019) found five alkaline compositions for lava flows occurring toward the bases of exposed sections within Chron 30N. They also obtained a low-TiO₂ composition for basalt from the top of the sequence.

We applied our age model to the samples of Haase et al. (2019) from their Mhow/Mandu section in the southern MP to determine ages for these samples (Figure 3). It is possible that some of their samples are from the same units sampled by us, implying some redundancy between the two data sets. The Mg# of Malwa basalts (Haase et al., 2019; present study) do not show a systematic age-related trend though the youngest sample exhibits the highest value in the section (Figure 4c). Ba/Nb ratios tend to increase upsection with most values >14 occurring after ~66.3 Ma (Figure 4a), whereas La/Lu values exhibit a negative trend with time with values <51 after 66.3 Ma (Figure 4b). When Malwa Plateau samples are plotted against dated samples from the Western Ghats, an opposite yet temporally overlapping trend in Ba/Nb with time can be observed, with Malwa samples indicating a positive trend and Western Ghats samples showing a negative trend (Figure 4d).

REE ratios from all samples in this study along with those from Haase et al. (2019) and Western Ghats samples reported by Basu et al. (2020) are plotted as La/Sm versus Sm/Yb (Figure 5). All samples from the Malwa Plateau plot at relatively high La/Sm, overlapping with Kalsubai (the oldest subgroup) rocks from the Western Ghats, but not with the field of Wai lavas (youngest subgroup) from the Western Ghats. However, Sr-Nd-Pb isotopic compositions of at least some of the Malwa basalts (Haase et al., 2019; Marzoli et al., 2022; Peng et al., 1998) are depleted (e.g., yield positive epsilon Nd values) and generally similar to those of Wai basalts from the Western

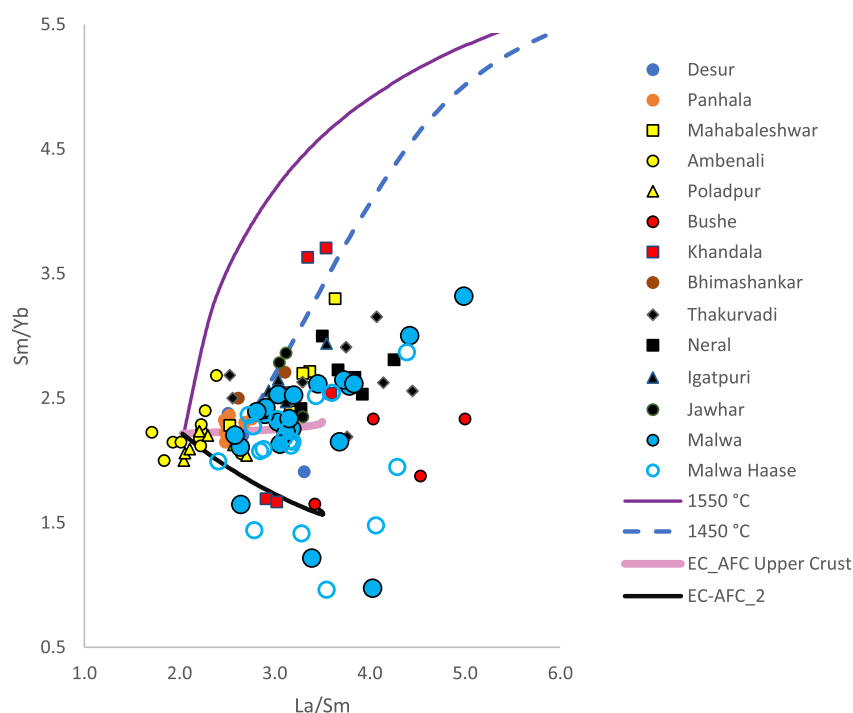


Figure 5. La/Sm versus Sm/Yb using samples from this study and from Haase et al. (2019), and Western Ghat samples reported in Basu et al. (2020). The solid purple and dashed blue curves represent REE trends for melts generated from a primitive anhydrous peridotite mantle at 1550 and 1450°C assuming a lithospheric thickness of 80 km using the REEBOX-PRO software package (Brown & Leshner, 2016). The thick pink line shows the REE variations modeled by energy-constrained recharge, assimilation, and fractional crystallization (EC-AFC) (Spera & Bohrsen, 2002). The highest La/Sm (3.5) of the calculated contaminated magma corresponds to a residual magma fraction of 0.9% and 3% assimilation of an average upper crust (Rudnick & Gao, 2003). The black line (EC-AFC_2) corresponds to the calculated composition of a magma that assimilated a hypothetical crustal rock in which Sm behaves compatibly, while La and Yb are incompatible. Details on the EC-AFC modeling are reported in Supporting Information S1.

Ghats. Few Malwa basalts trend to Sm/Yb values lower than basalts from the Western Ghats Lonavala subgroup basalts (Figure 5). Finally, Malwa alkaline basalts, particularly the trachybasalt MAL19-2, yield very high La/Sm and Sm/Yb and plot off the field of other Malwa and Western Ghats basalts.

DFA results on geochemical data for our samples and those of Haase et al. (2019) return some correlatives to Western Ghats chemotypes though several Malwa samples do not reliably match with any chemotype (Figure 6). Most samples that return a reasonable chemical correlation to a Western Ghat chemotype are vastly different in terms of their age relative to its counterpart in the main Deccan Plateau (Figure 6). Moreover, significant differences are evidenced in the succession of chemotypes. For example, low-TiO₂ basalts with high Ba/Nb are typical of the topmost Malwa flows, whereas such compositions characterize the Lonavala subgroup that occurs in the central part of the Western Ghats succession.

5. Discussion

5.1. Rates of Chemical Variability

Basalts of the Malwa Plateau record temporal chemical variations which can be quantified using results of the age model generated from our dated samples. Alkaline compositions at the base of exposed sections erupted within Chron 30N (Haase et al., 2019; Schöbel et al., 2014) and assuming accurate placement of the Chron 30N/29R boundary by Schöbel et al. (2014), the transition to solely tholeiitic compositions occurs after the first 500,000 years of eruptions. Overall, time-related positive trends in Ba/Nb and negative trends in La/Lu exist across the southern escarpment and are consistent with data presented in Haase et al. (2019) (Figure 4). The majority of lavas with the lowest values of Ba/Nb overlap with Reunion ocean island hot-spot basalt compositions (Haase et al., 2019) and erupted quasi-continuously over a period of ~350,000 years (Figure 3). After this, the

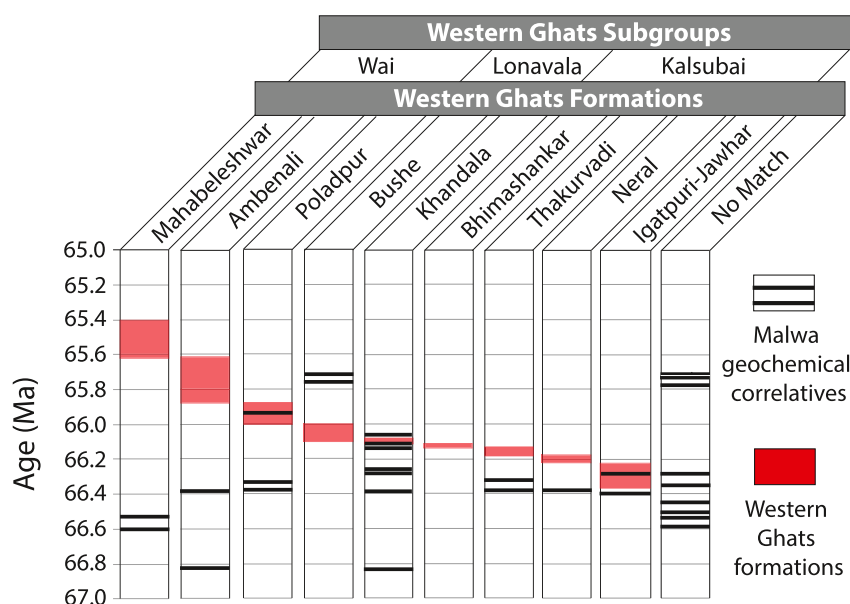


Figure 6. Geochemical comparison of Malwa Plateau and Western Ghats basalts formational assignments according to discriminant function analysis plotted against age. Red regions represent Western Ghats formations with appropriate names at the top of each column. Horizontal black lines represent samples presented in this study as well as results from previous Malwa Plateau studies that list relevant chemical and elevational data to be assigned a DFA output and an age according to the age model presented in this study. Samples with a Mahalanobis distance greater than 20 plots in the far right column labeled as “No Match.”

Malwa Plateau records ~700,000 years of progressive increases in Ba/Nb and decreases in La/Lu, with youngest samples the most enriched in $^{87}\text{Sr}/^{86}\text{Sr}$, MgO, and Sc. These chemical variations are possibly the result of the assimilation of various crustal rocks. However, the time-related decrease in the LREE/HREE ratios coupled with higher contents of compatible elements (e.g., MgO, Sc) cannot be modeled as a simple fractional crystallization process from a basaltic magma with Réunion-like compositions combined with assimilation of typical upper or lower crustal compositions (e.g., Rudnick & Gao, 2003). A crustal component involved in the genesis of the youngest Malwa magmas may be mafic rocks with residual amphibole and without residual garnet to account for the low ratios of La/Lu, Sm/Yb, and Nb/La (Figure 5). Similar conclusions were reached by Haase et al. (2019). The youngest Malwa basalts also overlap with Bushe basalts from the Western Ghats in low TiO_2 contents and enriched Sr-Nd isotopic compositions. However, the two groups of contaminated basalts are clearly distinct in terms of Pb isotopic compositions (Basu et al., 2020; Haase et al., 2019; Peng et al., 1998), suggesting that they were contaminated by distinct crustal rocks.

5.2. On Chemical Correlations of the Malwa Plateau to the Western Ghats

Chemostratigraphic characterizations within the Deccan province have greatly improved the understanding of unique flow fields and the ability to correlate monotonous basalts across large distances. The adoption of the Beane et al. (1986) chemical classification was driven by similar successes in correlating units within the Columbia River Basalts (Reidel et al., 2013; Swanson et al., 1979). Based on elemental ratios and radiogenic isotopes of Sr, Nd, Pb, and Hf, these classifications have been used to successfully identify formational boundaries over wide ranges of the Western Ghats though their application to flows and dikes of the various subprovinces is tenuous (Haase et al., 2019; Peng et al., 1998; Rao et al., 1985; Vanderkluisen et al., 2011). Despite the inconsistencies, contemporary studies remain tied to the chemostratigraphy established in the Western Ghats when making broad statements about the LIP as a whole (Basu et al., 2020; Eddy et al., 2020). $^{40}\text{Ar}/^{39}\text{Ar}$ dating results paired with traditional chemical DFA serve as a direct test on the validity of relating Western Ghats chemostratigraphy to outlying subprovinces as well as the hypothesis of southward-migrating volcanism (e.g., Devey & Lightfoot, 1986; Model B in Mitchell and Widdowson (1991), Schoene et al. (2019), and Eddy et al. (2020)). Samples at higher elevations (>500 m) from the top three Malwa formations return reasonable DFA correlations to Lonavala subgroup chemotypes of the Bushe and Khandala formations from the Western Ghats, in the “correct” stratigraphic order.

However, Khandala-like compositions can be found down section all the way to the base, underlying two Igatpuri/Jawhar correlative lavas and five lavas that have no reasonable correlative with any Western Ghats Formation, that is, samples over 20 standard deviations from the defined distribution. Additionally, lavas with matches to the Mahabaleshwar and Poladpur Formations occur out of order with respect to the Western Ghats lavas. Sample KOL20-1, the second oldest and most northerly sample analyzed, returns a reasonable match to the Ambenali chemotype, though is much older than any Western Ghats Ambenali lavas. Overall, the timing of chemical types defined through DFA is dramatically different between the Malwa Plateau and the Western Ghats, with Khandala chemotypes erupted earlier (66.8–66.2 Ma) in Malwa versus 66.2–66.1 Ma in the Western Ghats, but Bushe-like lavas erupted slightly later (65.9–65.8 Ma) in Malwa versus 66.1–66.0 Ma in the Western Ghats. These comparisons are based on the $^{40}\text{Ar}/^{39}\text{Ar}$ dates of Sprain et al. (2019) in preference to the U-Pb dates of Schoene et al. (2019) to eliminate intercalibration uncertainties between the two dating methods. Additionally, in Malwa, we have Poladpur-type and Mahabaleshwar-type lavas erupting significantly earlier than their counterparts in the Western Ghats.

Data presented in this study have confirmed that almost every Western Ghats chemotype aside from the Bhimashankar Formation can be found in the Malwa Plateau based on liberal (Mahalanobis Distance <20) DFA criteria, although, as noted by Haase et al. (2019), differences in Ti, Zr/Y, and Nb/La among potential DFA matches cast doubt on almost every correlation. These differences along with two trends in Sr and Nd isotope space led Haase et al. (2019) to speculate that three potential geochemical end member compositions contributed to magma genesis within the Malwa Plateau. Perhaps the most important end-member inferred by Haase et al. (2019) was that containing low ratios of Ce/Yb and Sm/Yb, that is, implicating assimilation of a garnet-free crustal rock type. This piece of evidence along with the data presented in this study strengthens the likelihood that various Deccan magmatic systems were controlled by similar processes but were chemically dependent on local shallow crustal compositions. The notion of province-wide shallow crustal interactions is further supported by evidence that megacrystic basalt marker units found across the entirety of the Deccan Traps resided in shallow crustal reservoirs (Marzoli et al., 2022). The Malwa Plateau sits on the Bundelkhand craton, which is overlain by shallow marine sediments of the Bijawar Group and Vindhyan Supergroup, shown by Kaila (1988) to be over a kilometer thick. Interaction with these chemically distinct cratons and the overlying supracrustal rocks is a potential source of chemical departures from Western Ghats chemotypes. Further analysis of radiogenic isotopes (e.g., Sr, Nd, Pb, Hf) from these formations would be useful to clarify the degree of primary magma source heterogeneity and lithospheric interaction.

5.3. Rare Earth Element Modeling

Overall trends in REE ratios suggest that Deccan lavas were sourced from mantle regions at varied temperatures. Wai subgroup lavas of the Mahabaleshwar, Ambenali, and Poladpur Formations of the Western Ghats are unique in that they yield low LREE enrichment, that is, low La/Sm that suggest high melt generation temperatures (Figure 5). With the forward mantle melting model REEBOX PRO (Brown & Leshner, 2016), we simulated adiabatic decompression melting of chemically homogeneous anhydrous peridotite at mantle temperatures of 1550 to 1450°C for a lithospheric thickness of 80 km compatible with geophysical studies (Saha et al., 2020). Details on the modeling are reported in Supporting Information S1.

Malwa samples presented in this study and in Haase et al. (2019) overlap more closely with Kalsubai than Wai subgroup lavas in terms of REE ratios. However, similar Sr-Nd-Pb isotopic compositions of several Malwa (Haase et al., 2019; Marzoli et al., 2022) and Wai basalts (Poladpur and Mahabaleshwar Formations, in particular; Basu et al., 2020; Peng et al., 1998) suggest a common mantle source for these tholeiites (Figure S6 in Supporting Information S1). Available Deccan basalt data, when compared to modeled REE curves, suggest slightly lower melt generation temperatures for Malwa compared to the Wai basalts of the Western Ghats (Figure 5). Though the REE ratios may be controlled to some degree by assimilation of the continental crust or from components from the lithospheric mantle, the latter is unlikely for Malwa and Wai basalts with similar isotopic compositions (Haase et al., 2019; Marzoli et al., 2022; Peng et al., 1998) and strengthens the case for slightly colder melting conditions in the North (Malwa) compared to the South (Western Ghats).

The only sample from our data set which shows strongly anomalous compositions (e.g., high Nb/La, high K_2O) is the alkaline trachybasalt MAL19-2. The REE ratios of this sample cannot be reproduced with the mantle melting model of Figure 5 and suggest significantly lower melting temperatures and possibly a distinct source

composition. We note that melting in the convecting mantle would not happen at temperatures less than 1450°C for a lithospheric thickness of 90 km or more. A possible interpretation for the composition of the trachybasalt MAL19-2 is that it was sourced from or contaminated by a sub-continental mantle lithosphere (Rao et al., 2020). Such sources are plausible as mafic alkaline and ultra-alkaline magmatism is widespread in the northern Deccan regions and within the Narmada rift (Basu et al., 2020; Dongre et al., 2022; Parisio et al., 2016).

5.4. Time-Related North-South Evolution of Deccan Magmatism

The overlap of Malwa major and minor element patterns with Western Ghats lavas can be explained through the lens of a mantle plume model in which a plume head impinges on the lithosphere wherein melt generation is established in localized zones that produce unique melts and relatively low magma volumes. It would therefore follow that the earliest and relatively low - temperature tholeiites and most alkaline melts would exist north of the main LIP, as the Indian craton continued moving north over the developing plume. Once the plume matured and established itself with major lithospheric conduits, one would expect higher eruptions rates and volumes such as are represented in the Western Ghats by the Wai subgroup.

In line with this notion, progressive increases in Ba/Nb over time in the Malwa Plateau are opposite to what is recorded in the Western Ghats using the available relevant data (Figure 4d). Dated and chemically analyzed Western Ghats samples exhibit decreasing values of Ba/Nb over a period of ~450,000 years that occurs when time correlative Malwa lavas are increasing in Ba/Nb. This eventual return to Réunion-like Ba/Nb values in the Western Ghats corresponds in time to Wai subgroup formations and the most voluminous flows in the Western Ghats. Furthermore, the presence of variable lava chemistries erupting at similar times are impossible to reconcile with a single evolving and southward-migrating eruptive center model but can be accounted for in a transcrustal model (Cashman et al., 2017; Mittal & Richards, 2021) in which multiple discrete magma reservoirs are variably connected throughout the laterally heterogeneous shallow crust. The occurrence of younger, relatively uncontaminated basalts in Ba/Nb space (Figure 4a) sampled by Haase et al. (2019) implies that smaller magma reservoirs were still being triggered by recharge associated overpressure within the Malwa Plateau despite the majority of overpressure having moved toward the Western Ghats at that time.

5.5. On Differences Between $^{40}\text{Ar}/^{39}\text{Ar}$ and U-Pb Ages

Contrasts in the overall timing of Malwa eruptions and those of the Western Ghats have implications for the dynamics of the Deccan system. As noted previously, the basal ~200 m of lava of the Mandleshwar and Kalisindh Formations in the southern part of the Malwa Plateau predate the oldest dated lavas of the Jawhar Fm. (~66.4 Ma; Sprain et al., 2019) in the Western Ghats by >400 ka. Thus, the inception of Deccan volcanism should be at least 66.8 Ma, which is a minimum depending on how much erupted basalt occurs in the present-day subsurface. While current dating methods applied to Western Ghats sequences have greatly improved the precision of Deccan eruptive timing, there remains disagreement between a “pulsed” (e.g., Schoene et al., 2015, 2019) versus “quasi-continuous” (e.g., Renne et al., 2015; Sprain et al., 2019) nature of eruptive tempo. Eddy et al. (2020) followed the approach of Schoene et al. (2019) and applied the U-Pb technique to zircons from red boles in MP sequences, using the Khadri (2003) formational nomenclature, and linked MP lavas to Pulse 1 of the four-pulse scenario inferred by Schoene et al. (2019). Chemical and radioisotopic age data from this study do not directly bear on the pulsed versus quasi-continuous eruptive tempo of the LIP as a whole, but do negate the validity of correlating Malwa Plateau eruptions to Pulse 1 of the Schoene et al. (2019) interpretation for the Western Ghats.

Many of the red boles sampled in Eddy et al. (2020) come from similar locations as basalts sampled in this study, and perhaps most notable is that the individual U-Pb and $^{40}\text{Ar}/^{39}\text{Ar}$ ages overlap significantly (Figure 7). Differences become more apparent when comparing U-Pb and $^{40}\text{Ar}/^{39}\text{Ar}$ model age results applied to two different calibrations of our $^{40}\text{Ar}/^{39}\text{Ar}$ age data at 95% confidence, when all systematic uncertainties in each method are considered (Figure 8). The U-Pb model ages are systematically younger or older than the $^{40}\text{Ar}/^{39}\text{Ar}$ model ages depending on calibration to Renne et al. (2011) or Kuiper et al. (2008), respectively (Figure 8). The offsets may be a result of miscalibration between the two dating methods, highlighting the need for further progress in intercalibration of the two geochronometers. If the Kuiper et al. (2008) calibration is more accurate, the Western Ghats age model inferred from red-bole zircon U-Pb data (Schoene et al., 2015, 2019) would be systematically 300–500 ka older than the $^{40}\text{Ar}/^{39}\text{Ar}$ ages (Renne et al., 2015; Sprain et al., 2019), clearly a much greater bias

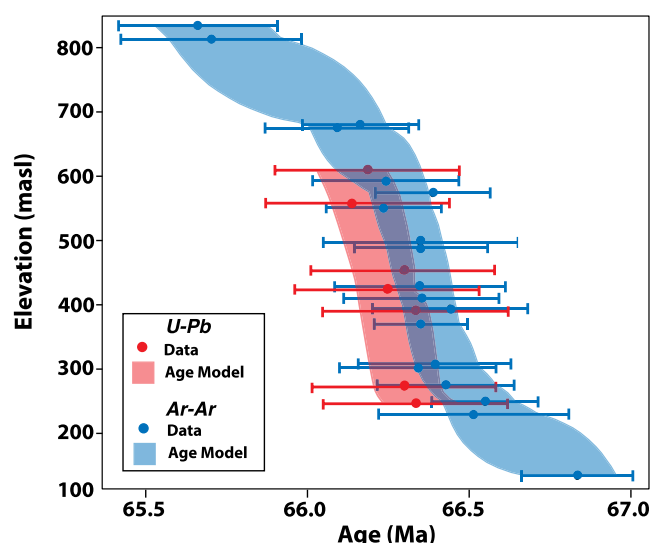


Figure 7. $^{40}\text{Ar}/^{39}\text{Ar}$ ages plotted as a function of elevation compared with U-Pb data reported in Eddy et al. (2020). Uncertainties for $^{40}\text{Ar}/^{39}\text{Ar}$ data points (blue) are 2σ including systematic uncertainties, age model bounds for $^{40}\text{Ar}/^{39}\text{Ar}$ data (blue region) are 95% confidence including systematic uncertainties. Uncertainties for U-Pb data points (red) are the 95% confidence of the youngest grain and include systematic uncertainties. The red region represents the preferred age model interpretation presented by Eddy et al. (2020).

eroding into the global marine system. The possibility that low Os concentrations in representative Deccan basalts may not account for global changes was posited by Allègre et al. (1999), but given the chemical and temporal heterogeneity of basalts within the Malwa Plateau shown in this study, as well as uncertain links to other northern subprovinces, a comprehensive re-evaluation of the Deccan Os contents is required for more robust links to global signals.

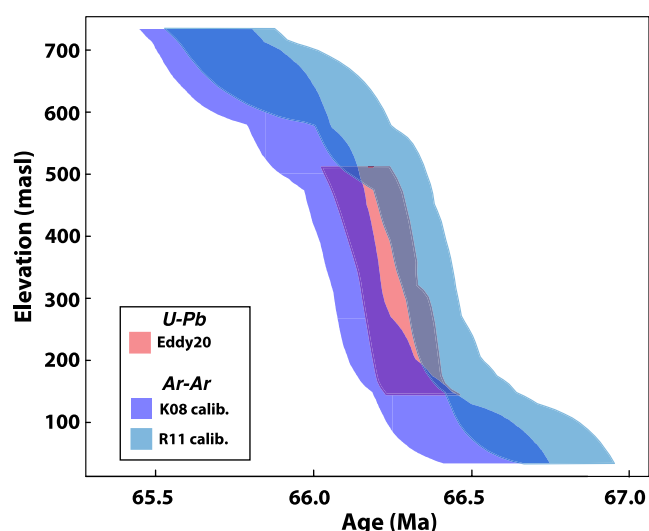


Figure 8. $^{40}\text{Ar}/^{39}\text{Ar}$ and U-Pb age models plotted as a function of elevation. $^{40}\text{Ar}/^{39}\text{Ar}$ age model results depict 95% confidence intervals including systematic uncertainties for data calibrated to Renne et al. (2011) in teal and Kuiper et al. (2008) in purple. The salmon region represents the preferred age model interpretation presented by Eddy et al. (2020).

than is evident in the MP. We hypothesize that because the Western Ghats are farther from putative silicic magma sources in the northwesternmost Deccan (Basu et al., 2020) than the Malwa Plateau, the more distal depositional sites were more prone to reworking of zircons prior to deposition in the red boles, hence biasing the results to spuriously old ages. Because age biases expected in this scenario would be variable, a further implication is that the case for major eruptive pulses (Schoene et al., 2019) would be undermined.

5.6. Paleoenvironmental Implications

The timing of main phase activity expressed in Malwa lavas is consistent with a linkage to Late Maastrichtian warming trends of 2–4°C from 66.7 to 66.1 Ma inferred from paleoenvironmental and biotic changes (Barrera et al., 1999; Li & Keller, 1998; Pearson et al., 2002; Wilf et al., 2003; Wilson, 2005), $\delta^{18}\text{O}$ benthic foraminifera records (Barnet et al., 2018; Hull et al., 2020), and clumped isotope temperature proxies (Tobin et al., 2014). Notably, the Malwa Plateau and lavas within the Narmada-Tapi rift are the only regions of the Deccan that rest on and probably contain heated sediments from a shale- and carbonate-bearing basin. Thermogenic carbon from the Vindhyan basin sediments may thus have contributed to the end-Maastrichtian warming. The initiation of activity within the Malwa Plateau also coincides with the reduction in the $^{187}\text{Os}/^{188}\text{Os}$ values of ocean sediments toward more radiogenic values (Ravizza & VonderHaar, 2012; Robinson et al., 2009), implying an increase in the mantle contribution. While the steepest and most apparent decline occurs within Chron 29R, sampling density at Bottaccione, Italy, suggests that multiple minor excursions to more radiogenic Os isotopic values occurred within Chron 30N and could be a result of Malwa basalts

6. Conclusions

New $^{40}\text{Ar}/^{39}\text{Ar}$ ages from basalt exposures of the Malwa Plateau record a million years of volcanic activity with the highest eruptive rates during a ~350,000-year period before the KPB. The oldest samples dated in this study indicate that effusive basaltic eruptions within the Malwa Plateau started significantly (i.e., at least ~400 ka) before the activity in the Western Ghats to the south and thus contribute to a plausible forcing mechanism for the Late Maastrichtian warming event. Age and chemical progressions across the LIP support the hypothesis that the Deccan Traps records the initiation and cessation of plume volcanism as the Indian subcontinent moved north over the Réunion hotspot, as put forth by several previous studies (e.g., Courtillot et al., 1986; Devey & Lightfoot, 1986; Richards et al., 1989). $^{40}\text{Ar}/^{39}\text{Ar}$ ages coupled with DFA results show significant temporal overlap between Malwa Plateau basalts and geochemically distinct basalts of the Western Ghats. Rare earth element trends coupled with inferred mantle source regions from the Malwa Plateau and Western Ghats lavas suggest that the earliest melts were generated as lower melt fractions at lower temperatures than the younger, more voluminous lavas typical of the Wai Subgroup. It is now clear that coeval Deccan eruptive centers were active throughout the Late Maastrichtian and that Malwa Plateau flows did not extend south of the Tapi River and the southern boundary of the Narmada Rift System.

Data Availability Statement

The data used in this paper can be found at Tholt (2023).

Acknowledgments

This work is dedicated to the memory of Abdur-Rahim Jaouni, whose skill and perseverance in sample preparation has been a part of countless contributions to the scientific community for the last half-century. Funding was supported by U.S. National Science Foundation Grants EAR-1615203 and EAR-1736737, the Ann and Gordon Getty Foundation, and the Esper S. Larsen Fund of the University of California, Berkeley. The authors would like to thank T. Mittal, T. Becker, and V. Kale for helpful discussions and assistance, and C. Sprain and D. Mark for constructive reviews of the manuscript.

References

- Alexander, P. O. (1981). *Age and duration of Deccan volcanism: K-Ar evidence* (pp. 244–258). Memoir-Geological Society of India.
- Allegre, C. J., Birck, J. L., Capmas, F., & Courtillot, V. (1999). Age of the Deccan traps using ^{187}Re – ^{187}Os systematics. *Earth and Planetary Science Letters*, 170(3), 197–204. [https://doi.org/10.1016/s0012-821x\(99\)00110-7](https://doi.org/10.1016/s0012-821x(99)00110-7)
- Barnet, J. S., Littler, K., Kroon, D., Leng, M. J., Westerhold, T., Röhl, U., & Zachos, J. C. (2018). A new high-resolution chronology for the Late Maastrichtian warming event: Establishing robust temporal links with the onset of Deccan volcanism. *Geology*, 46(2), 147–150. <https://doi.org/10.1130/g39771.1>
- Barrera, E., Savin, S. M., & Johnson, C. C. (1999). *Evolution of late Campanian-Maastrichtian marine climates and oceans* (pp. 245–282). Special Papers-Geological Society of America.
- Basu, A. R., Chakrabarty, P., Sztmanowski, D., Ibañez-Mejia, M., Schoene, B., Ghosh, N., & Georg, R. B. (2020). Widespread silicic and alkaline magmatism synchronous with the Deccan Traps flood basalts, India. *Earth and Planetary Science Letters*, 552, 116616. <https://doi.org/10.1016/j.epsl.2020.116616>
- Basu, A. R., Renne, P. R., DasGupta, D. K., Teichmann, F., & Poreda, R. J. (1993). Early and late alkali igneous pulses and a high- ^3He plume origin for the Deccan flood basalts. *Science*, 261(5123), 902–906. <https://doi.org/10.1126/science.261.5123.902>
- Beane, J. E., Turner, C. A., Hooper, P. R., Subbarao, K. V., & Walsh, J. N. (1986). Stratigraphy, composition and form of the Deccan basalts, Western Ghats, India. *Bulletin of Volcanology*, 48(1), 61–83. <https://doi.org/10.1007/bf01073513>
- Bhalla, M. S., & Rao, G. V. S. P. (1974). Low field hysteresis and palaeomagnetic stability criterion of rock samples from Dhar (Deccan traps) India. *Journal of Indian Geophysical Union*, 12, 14–21.
- Brown, E. L., & Leshner, C. E. (2016). REEBOX PRO: A forward model simulating melting of thermally and lithologically variable upwelling mantle. *Geochemistry, Geophysics, Geosystems*, 17(10), 3929–3968. <https://doi.org/10.1002/2016gc006579>
- Callegaro, S., Baker, D. R., Renne, P. R., Melluso, L., Geraki, K., Whitehouse, M. J., et al. (2023). Recurring volcanic winters during the latest Cretaceous: Sulfer and fluorine budgets of the Deccan Traps lavas. *Science Advances*, 9(40). <https://doi.org/10.1126/sciadv.adg8284>
- Cashman, K. V., Sparks, R. S. J., & Blundy, J. D. (2017). Vertically extensive and unstable magmatic systems: A unified view of igneous processes. *Science*, 355(6331), eaag3055. <https://doi.org/10.1126/science.aag3055>
- Chen, A. L., Quidelleur, X., Fluteau, F., Courtillot, V., & Bajpai, S. (2007). ^{40}K – ^{40}Ar dating of the Main Deccan large igneous province: Further evidence of KTB age and short duration. *Earth and Planetary Science Letters*, 263(1–2), 1–15. <https://doi.org/10.1016/j.epsl.2007.07.011>
- Courtillot, V., Besse, J., Vandamme, D., Montigny, R., Jaeger, J., & Cappetta, H. (1986). Deccan flood basalts at the Cretaceous/Tertiary boundary? *Earth and Planetary Science Letters*, 80(3–4), 361–374. [https://doi.org/10.1016/0012-821x\(86\)90118-4](https://doi.org/10.1016/0012-821x(86)90118-4)
- Courtillot, V., Feraud, G., Maluski, H., Vandamme, D., Moreau, M. G., & Besse, J. (1988). Deccan flood basalts and the Cretaceous/Tertiary boundary. *Nature*, 333(6176), 843–846. <https://doi.org/10.1038/333843a0>
- Devey, C. W., & Lightfoot, P. C. (1986). Volcanological and tectonic control of stratigraphy and structure in the western Deccan traps. *Bulletin of Volcanology*, 48(4), 195–207. <https://doi.org/10.1007/BF01087674>
- Dongre, A., Dhote, P. S., Zamarkar, P., Sangode, S. J., Belyanin, G., Meshram, D. C., et al. (2022). Short-lived alkaline magmatism related to the Réunion plume in the Deccan large igneous province: Inferences from petrology, $^{40}\text{Ar}/^{39}\text{Ar}$ geochronology and palaeomagnetism of lamprophyre from the Sarnu-Dandali alkaline igneous complex. In L. Krmiček, & N. V. Chalapathi Rao (Eds.), *Lamprophyres, lamproites and related rocks: Tracers to supercontinent cycles and metallogenesis*. Geological Society of London. <https://doi.org/10.1144/SP513-2021-34>
- Duncan, R. A., & Pyle, D. G. (1988). Rapid eruption of the Deccan flood basalts at the Cretaceous/Tertiary boundary. *Nature*, 333(6176), 841–843. <https://doi.org/10.1038/333841a0>
- Eddy, M. P., Schoene, B., Samperton, K. M., Keller, G., Adatte, T., & Khadri, S. F. (2020). U-Pb zircon age constraints on the earliest eruptions of the Deccan Large Igneous Province, Malwa Plateau, India. *Earth and Planetary Science Letters*, 540, 116249. <https://doi.org/10.1016/j.epsl.2020.116249>
- Fendley, I. M., Mittal, T., Sprain, C. J., Marvin-DiPasquale, M., Tobin, T. S., & Renne, P. R. (2019). Constraints on the volume and rate of Deccan Traps flood basalt eruptions using a combination of high-resolution terrestrial mercury records and geochemical box models. *Earth and Planetary Science Letters*, 524, 115721. <https://doi.org/10.1016/j.epsl.2019.115721>
- Geological Survey of India. (1993). Published Quadrangle Geological Map, Map Printing Division, Geological Survey of India, Government of India Publications.
- Haase, K., Regelous, M., Schöbel, S., Günther, T., & de Wall, H. (2019). Variation of melting processes and magma sources of the early Deccan flood basalts, Malwa Plateau, India. *Earth and Planetary Science Letters*, 524, 115711. <https://doi.org/10.1016/j.epsl.2019.115711>
- Hernandez Nava, A., Black, B. A., Gibson, S. A., Bodnar, R. J., Renne, P. R., & Vanderkluyden, L. (2021). Reconciling early Deccan Traps CO_2 outgassing and pre-KPB global climate. *Proceedings of the National Academy of Sciences of the United States of America*, 118(14), e2007797118. <https://doi.org/10.1073/pnas.2007797118>
- Hofmann, C., Feraud, G., & Courtillot, V. (2000). $^{40}\text{Ar}/^{39}\text{Ar}$ dating of mineral separates and whole rocks from the Western Ghats lava pile: Further constraints on duration and age of the Deccan traps. *Earth and Planetary Science Letters*, 180(1–2), 13–27. [https://doi.org/10.1016/s0012-821x\(00\)00159-x](https://doi.org/10.1016/s0012-821x(00)00159-x)
- Hooper, P., Widdowson, M., & Kelley, S. (2010). Tectonic setting and timing of the final Deccan flood basalt eruptions. *Geology*, 38(9), 839–842. <https://doi.org/10.1130/g31072.1>
- Hull, P. M., Bornemann, A., Penman, D. E., Henehan, M. J., Norris, R. D., Wilson, P. A., et al. (2020). On impact and volcanism across the Cretaceous-Paleogene boundary. *Science*, 367(6475), 266–272. <https://doi.org/10.1126/science.aay5055>
- Jay, A. E., & Widdowson, M. (2008). Stratigraphy, structure and volcanology of the se Deccan continental flood basalt province: Implications for eruptive extent and volumes. *Journal of the Geological Society*, 165(1), 177–188. <https://doi.org/10.1144/0016-76492006-062>
- Kaila, K. L. (1988). Mapping the thickness of Deccan Trap flows in India from DSS studies and interferences about a hidden Mesozoic Basin in the Narmada-Tapi Region. In K. V. Subbarao (Ed.), *Deccan flood basalts, Memoir - Geologic Society of India* (Vol. 10, pp. 91–116).
- Kale, V. S., Dole, G., Shandilya, P., & Pande, K. (2020). Stratigraphy and correlations in Deccan Volcanic Province, India: Quo Vadis? *GSA Bulletin*, 132(3–4), 588–607. <https://doi.org/10.1130/b35018.1>
- Kaneoka, I., & Haramura, H. (1973). K/Ar ages of successive lava flows from the Deccan Traps, India. *Earth and Planetary Science Letters*, 18(2), 229–236. [https://doi.org/10.1016/0012-821x\(73\)90061-7](https://doi.org/10.1016/0012-821x(73)90061-7)

- Keller, C. B. (2018). Chron.jl: A Bayesian framework for integrating eruption age and age-depth modelling. <https://doi.org/10.17605/osf.io/TQX3F>
- Khadri, S. F. R. (2003). Occurrence of N–R–N sequence in the Malwa Deccan lava flows to the north of Narmada region, Madhya Pradesh, India. *Current Science*, 85(8), 1126–1129.
- Khadri, S. F. R., & Nagar, R. G. (1994). *Magnetostratigraphy of Malwa Deccan Traps Near Mandu Region, Madhya Pradesh* (pp. 199–210). Memoirs-Geological Society of India.
- Krishnamurthy, P. (2020). The Deccan volcanic province (DVP), India: A review. *Journal of the Geological Society of India*, 96(1), 9–35. <https://doi.org/10.1007/s12594-020-1501-5>
- Kuiper, K. F., Deino, A., Hilgen, F. J., Krijgsman, W., Renne, P. R., & Wijbrans, J. R. (2008). Synchronizing rock clocks of Earth history. *Science*, 320(5875), 500–504. <https://doi.org/10.1126/science.1154339>
- Li, L., & Keller, G. (1998). Abrupt deep-sea warming at the end of the Cretaceous. *Geology*, 26(11), 995–998. [https://doi.org/10.1130/0091-7613\(1998\)026<0995:adswat>2.3.co;2](https://doi.org/10.1130/0091-7613(1998)026<0995:adswat>2.3.co;2)
- Marzoli, A., Renne, P. R., Andreasen, R., Spiess, R., Chiaradia, M., Ruth, D. C., et al. (2022). The shallow magmatic plumbing system of the Deccan Traps, evidence from plagioclase megacrysts and their host lavas. *Journal of Petrology*, 63(9), egac075. <https://doi.org/10.1093/ptrology/egac075>
- McLean, D. M. (1985). Deccan traps mantle degassing in the terminal Cretaceous marine extinctions. *Cretaceous Research*, 6(3), 235–259. [https://doi.org/10.1016/0195-6671\(85\)90048-5](https://doi.org/10.1016/0195-6671(85)90048-5)
- Mitchell, C., & Widdowson, M. (1991). A geological map of the southern Deccan Traps, India and its structural implications. *Journal of the Geological Society*, 148(3), 495–505. <https://doi.org/10.1144/gsjgs.148.3.0495>
- Mittal, T., & Richards, M. A. (2021). The magmatic architecture of continental flood basalts: 2. A new conceptual model. *Journal of Geophysical Research: Solid Earth*, 126(12), e2021JB021807. <https://doi.org/10.1029/2021jb021807>
- Mohabey, D. M., & Samant, B. (2013). *Deccan continental flood basalt eruption terminated Indian dinosaurs before the Cretaceous-Paleogene boundary* (Vol. 1, pp. 260–267). Geological Society of India Special Publication.
- Pande, K., Pattanayak, S. K., Subbarao, K. V., Navaneethakrishnan, P., & Venkatesan, T. R. (2004). $^{40}\text{Ar}/^{39}\text{Ar}$ age of a lava flow from the Bhimashankar Formation, Giravali Ghat, Deccan Traps. *Journal of Earth System Science*, 113(4), 755–758. <https://doi.org/10.1007/bf02704034>
- Parisio, L., Jourdan, F., Marzoli, A., Melluso, L., Sethna, S. F., & Bellieni, G. (2016). $^{40}\text{Ar}/^{39}\text{Ar}$ ages of alkaline and tholeiitic rocks from the northern Deccan Traps: Implications for magmatic processes and the K–Pg boundary. *Journal of the Geological Society*, 173(4), 679–688. <https://doi.org/10.1144/jgs2015-133>
- Pearson, R. G., Dawson, T. P., Berry, P. M., & Harrison, P. A. (2002). SPECIES: A spatial evaluation of climate impact on the envelope of species. *Ecological Modelling*, 154(3), 289–300. [https://doi.org/10.1016/s0304-3800\(02\)00056-x](https://doi.org/10.1016/s0304-3800(02)00056-x)
- Peng, Z. X., Mahoney, J. J., Hooper, P. R., Macdougall, J. D., & Krishnamurthy, P. (1998). Basalts of the northeastern Deccan Traps, India: Isotopic and elemental geochemistry and relation to southwestern Deccan stratigraphy. *Journal of Geophysical Research*, 103(B12), 29843–29865. <https://doi.org/10.1029/98jb01514>
- Rao, M. S., Reddy, N. R., Subbarao, K. V., Prasad, C. V. R. K., & Radhakrishnamurthy, C. (1985). Chemical and magnetic stratigraphy of parts of Narmada region, Deccan basalt province. *Geological Society of India*, 26(9), 617–639.
- Rao, N. V. C., Giri, R. K., Sharma, A., & Pandey, A. (2020). Lamprophyres from the Indian shield: A review of their occurrence, petrology, tectonomagmatic significance and relationship with the Kimberlites and related rocks. *Episodes Journal of International Geoscience*, 43(1), 231–248. <https://doi.org/10.18814/epiugs/2020/020014>
- Ravizza, G., & VonderHaar, D. (2012). A geochemical clock in earliest Paleogene pelagic carbonates based on the impact-induced Os isotope excursion at the Cretaceous-Paleogene boundary. *Paleoceanography*, 27(3), PA3219. <https://doi.org/10.1029/2012pa002301>
- Ray, R., Sheth, H. C., & Mallik, J. (2007). Structure and emplacement of the Nandurbar–Dhule mafic dyke swarm, Deccan Traps, and the tectonomagmatic evolution of flood basalts. *Bulletin of Volcanology*, 69(5), 537–551. <https://doi.org/10.1007/s00445-006-0089-y>
- Reidel, S. P., Camp, V. E., Tolan, T. L., & Martin, B. S. (2013). The Columbia River flood basalt province: Stratigraphy, areal extent, volume, and physical volcanology. *Geological Society of America Special Paper*, 497, 1–43.
- Renne, P. R., Balco, G., Ludwig, K. R., Mundil, R., & Min, K. (2011). Response to the comment by WH Schwarz et al. on “Joint determination of 40K decay constants and $^{40}\text{Ar}/^{40}\text{K}$ for the Fish Canyon sanidine standard, and improved accuracy for $^{40}\text{Ar}/^{39}\text{Ar}$ geochronology” by PR Renne et al. (2010). *Geochimica et Cosmochimica Acta*, 75(17), 5097–5100. <https://doi.org/10.1016/j.gca.2011.06.021>
- Renne, P. R., Sprain, C. J., Richards, M. A., Self, S., Vanderkluysen, L., & Pande, K. (2015). State shift in Deccan volcanism at the Cretaceous-Paleogene boundary, possibly induced by impact. *Science*, 350(6256), 76–78. <https://doi.org/10.1126/science.aac7549>
- Richards, M., Alvarez, W., Self, S., Karlstrom, L., Renne, P. R., Manga, M., et al. (2015). Triggering of the largest Deccan eruptions by the Chicxulub impact. *Bulletin of the Geological Society of America*, 127(11–12), 1507–1520. <https://doi.org/10.1130/B31167.1>
- Richards, M. A., Duncan, R. A., & Courtillot, V. E. (1989). Flood basalts and hot-spot tracks: Plume heads and tails. *Science*, 246(4926), 103–107. <https://doi.org/10.1126/science.246.4926.103>
- Robinson, N., Ravizza, G., Coccioni, R., Peucker-Ehrenbrink, B., & Norris, R. (2009). A high-resolution marine $^{187}\text{Os}/^{188}\text{Os}$ record for the Late Maastrichtian: Distinguishing the chemical fingerprints of Deccan volcanism and the KP impact event. *Earth and Planetary Science Letters*, 281(3–4), 159–168. <https://doi.org/10.1016/j.epsl.2009.02.019>
- Rudnick, R. L., & Gao, S. (2003). Composition of the continental crust. In R. L. Rudnick (Ed.), *The crust, Treatise on geochemistry* (Vol. 3, pp. 1–64). Elsevier.
- Saha, G. K., Prakasam, K. S., & Rai, S. S. (2020). Diversity in the peninsular Indian lithosphere revealed from ambient noise and earthquake tomography. *Physics of the Earth and Planetary Interiors*, 306, 106523. <https://doi.org/10.1016/j.pepi.2020.106523>
- Schöbel, S., de Wall, H., Ganerød, M., Pandit, M. K., & Rolf, C. (2014). Magnetostratigraphy and $^{40}\text{Ar}/^{39}\text{Ar}$ geochronology of the Malwa Plateau region (Northern Deccan Traps), central western India: Significance and correlation with the main Deccan Large Igneous Province sequences. *Journal of Asian Earth Sciences*, 89, 28–45. <https://doi.org/10.1016/j.jseaes.2014.03.022>
- Schoene, B., Eddy, M. P., Samperton, K. M., Keller, C. B., Keller, G., Adatte, T., & Khadri, S. F. (2019). U–Pb constraints on pulsed eruption of the Deccan Traps across the end-Cretaceous mass extinction. *Science*, 363(6429), 862–866. <https://doi.org/10.1126/science.aau2422>
- Schoene, B., Samperton, K. M., Eddy, M. P., Keller, G., Adatte, T., Bowring, S. A., & Gertsch, B. (2015). U–Pb geochronology of the Deccan Traps and relation to the end-Cretaceous mass extinction. *Science*, 347(6218), 182–184. <https://doi.org/10.1126/science.aaa0118>
- Self, S., Mittal, T., Dole, G., & Vanderkluysen, L. (2022). Toward understanding Deccan volcanism. *Annual Review of Earth and Planetary Sciences*, 50(1), 477–506. <https://doi.org/10.1146/annurev-earth-012721-051416>
- Self, S., Widdowson, M., Thordarson, T., & Jay, A. E. (2006). Volatile fluxes during flood basalt eruptions and potential effects on the global environment: A Deccan perspective. *Earth and Planetary Science Letters*, 248(1–2), 518–532. <https://doi.org/10.1016/j.epsl.2006.05.041>

- Shanker, R. (1991). Thermal and crustal structure of "SONATA." A zone of mid continental rifting in Indian shield. *Geological Society of India*, 37(3), 211–220.
- Sheth, H. C., Zellmer, G. F., Kshirsagar, P. V., & Cucciniello, C. (2013). Geochemistry of the Palitana flood basalt sequence and the Eastern Saurashtra dykes, Deccan Traps: Clues to petrogenesis, dyke–flow relationships, and regional lava stratigraphy. *Bulletin of Volcanology*, 75(4), 1–23. <https://doi.org/10.1007/s00445-013-0701-x>
- Singh, A. K., & Chakraborty, P. P. (2022). Shales of Palaeo-Mesoproterozoic Vindhyan Basin, central India: Insight into sedimentation dynamics of Proterozoic shelf. *Geological Magazine*, 159(2), 247–268. <https://doi.org/10.1017/S00167568200011683>
- Spera, F. J., & Bohrsen, W. A. (2001). Energy-constrained open-system magmatic processes I: General model and energy-constrained assimilation and fractional crystallization (EC-AFC) formulation. *Journal of Petrology*, 42(5), 999–1018. <https://doi.org/10.1093/ptrology/42.5.999>
- Sprain, C. J., Renne, P. R., Clemens, W. A., & Wilson, G. P. (2018). Calibration of chron C29r: New high-precision geochronologic and paleomagnetic constraints from the Hell Creek region, Montana. *GSA Bulletin*, 130(9–10), 1615–1644. <https://doi.org/10.1130/B31890.1>
- Sprain, C. J., Renne, P. R., Vanderkluyzen, L., Pande, K., Self, S., & Mittal, T. (2019). The eruptive tempo of Deccan volcanism in relation to the Cretaceous–Paleogene boundary. *Science*, 363(6429), 866–870. <https://doi.org/10.1126/science.aav1446>
- Sprain, C. J., Renne, P. R., Wilson, G. P., & Clemens, W. A. (2015). High-resolution chronostratigraphy of the terrestrial Cretaceous–Paleogene transition and recovery interval in the Hell Creek region, Montana. *Bulletin*, 127(3–4), 393–409. <https://doi.org/10.1130/b31076.1>
- Sun, S.-S., & McDonough, W. F. (1989). Chemical and isotopic systematics of oceanic basalts: Implications for mantle composition and processes. In A. D. Saunders, & M. J. Norry (Eds.), *Magmatism in the ocean basins* (Vol. 42, pp. 313–345). Geological Society, London, UK: Special Publications.
- Sun, S.-S., Nesbitt, R. W., & Sharaskin, A. Y. (1979). Geochemical characteristics of mid-ocean ridge basalts. *Earth and Planetary Science Letters*, 44(1), 119–138. [https://doi.org/10.1016/0012-821X\(79\)90013-X](https://doi.org/10.1016/0012-821X(79)90013-X)
- Swanson, D., Wright, T., Hooper, P., & Bentley, R. (1979). Revisions in stratigraphic nomenclature of the Columbia River basalt group. Tech. Bulletin 1457-G, US Geological Survey.
- Tholt, A. (2023). Geochronological constraints on the evolution and petrogenesis of the Malwa Plateau subprovince of the Deccan Traps [Dataset]. Zenodo. <https://doi.org/10.5281/zenodo.10092452>
- Tobin, T. S., Wilson, G. P., Eiler, J. M., & Hartman, J. H. (2014). Environmental change across a terrestrial Cretaceous–Paleogene boundary section in eastern Montana, USA, constrained by carbonate clumped isotope paleothermometry. *Geology*, 42(4), 351–354. <https://doi.org/10.1130/G35262.1>
- Valdiya, K. S., & Sanwal, J. (2017). India: An assemblage of multiple terranes. In *Developments in Earth surface processes* (Vol. 22, pp. 15–29). Elsevier.
- Vandamme, D., Courtillot, V., Besse, J., & Montigny, R. (1991). Paleomagnetism and age determinations of the Deccan Traps (India): Results of a Nagpur–Bombay Traverse and review of earlier work. *Reviews of Geophysics*, 29(2), 159–190. <https://doi.org/10.1029/91rg00218>
- Vanderkluyzen, L., Mahoney, J. J., Hooper, P. R., Sheth, H. C., & Ray, R. (2011). The feeder system of the Deccan Traps (India): Insights from dike geochemistry. *Journal of Petrology*, 52(2), 315–343. <https://doi.org/10.1093/ptrology/egq082>
- Verma, O., & Khosla, A. (2019). Developments in the stratigraphy of the Deccan Volcanic Province, peninsular India. *Comptes Rendus Geoscience*, 351(7), 461–476. <https://doi.org/10.1016/j.crte.2019.10.002>
- Verma, R. K., & Banerjee, P. (1992). Nature of continental crust along the Narmada—Son Lineament inferred from gravity and deep seismic sounding data. *Tectonophysics*, 202(2–4), 375–397. [https://doi.org/10.1016/0040-1951\(92\)90121-1](https://doi.org/10.1016/0040-1951(92)90121-1)
- Wellman, P., & McElhinny, M. W. (1970). K–Ar age of the Deccan traps, India. *Nature*, 227(5258), 595–596. <https://doi.org/10.1038/227595a0>
- Westerhold, T., Marwan, N., Drury, A. J., Liebrand, D., Agnini, C., Anagnostou, E., et al. (2020). An astronomically dated record of Earth's climate and its predictability over the last 66 million years. *Science*, 369(6509), 1383–1387. <https://doi.org/10.1126/science.aba6853>
- Wilf, P., Johnson, K. R., & Huber, B. T. (2003). Correlated terrestrial and marine evidence for global climate changes before mass extinction at the Cretaceous–Paleogene boundary. *Proceedings of the National Academy of Sciences of the United States of America*, 100(2), 599–604. <https://doi.org/10.1073/pnas.0234701100>
- Wilson, G. P. (2005). Mammalian faunal dynamics during the last 1.8 million years of the Cretaceous in Garfield County, Montana. *Journal of Mammalian Evolution*, 12(1), 53–76. <https://doi.org/10.1007/s10914-005-6943-4>
- Zeebe, R. E. (2012). LOSCAR: Long-term ocean-atmosphere-sediment carbon cycle reservoir model v2. 0.4. *Geoscientific Model Development*, 5(1), 149–166. <https://doi.org/10.5194/gmd-5-149-2012>

References From the Supporting Information

- McDonough, W. F., & Sun, S.-S. (1995). The composition of the Earth. *Chemical Geology*, 120(3), 223–253. [https://doi.org/10.1016/0009-2541\(94\)00140-4](https://doi.org/10.1016/0009-2541(94)00140-4)
- Peng, Z. X., Mahoney, J., Hooper, P., Harris, C., & Beane, J. (1994). A role for lower continental crust in flood basalt genesis? Isotopic and incompatible element study of the lower six formations of the western Deccan Traps. *Geochimica et Cosmochimica Acta*, 58(1), 267–288. [https://doi.org/10.1016/0016-7037\(94\)90464-2](https://doi.org/10.1016/0016-7037(94)90464-2)
- Spera, F. J., & Bohrsen, W. A. (2002). Energy-constrained open-system magmatic processes 3. Energy-constrained recharge, assimilation, and fractional crystallization (EC-RAFC). *Geochemistry, Geophysics, Geosystems*, 3(12), 1–20. <https://doi.org/10.1029/2002GC000315>